

1 **Simultaneous reductions in emissions of black carbon and co-emitted species will**  
2 **weaken the aerosol net cooling effect**

3

4 Z. L. Wang<sup>1,2</sup>, H. Zhang<sup>3,2</sup>, and X. Y. Zhang<sup>1,4</sup>

5 <sup>1</sup>Chinese Academy of Meteorological Sciences, Beijing, China

6 <sup>2</sup>Collaborative Innovation Center on Forecast and Evaluation of Meteorological  
7 Disasters, Nanjing University of Information Science and Technology, Nanjing, China

8 <sup>3</sup>Laboratory for Climate Studies, National Climate Center, China Meteorological  
9 Administration, Beijing, China

10 <sup>4</sup>Key Laboratory for Atmospheric Chemistry, Chinese Academy of Meteorological  
11 Sciences, Beijing, China

12 Correspondence to: X. Y. Zhang (xiaoye@cams.cma.gov.cn)

13

14 **Abstract**

15 Black carbon (BC), a distinct type of carbonaceous material formed from the  
16 incomplete combustion of fossil and biomass based fuels under certain conditions, can  
17 interact with solar radiation and clouds through its strong light-absorption ability,  
18 thereby warming the Earth's climate system. Some studies have even suggested that  
19 global warming could be slowed down in the short term by eliminating BC emission  
20 due to its short lifetime. In this study, we estimate the influence of removing some  
21 sources of BC and other co-emitted species on the aerosol radiative effect by using an  
22 aerosol-climate atmosphere-only model BCC\_AGCM2.0.1\_CUACE/Aero with

23 prescribed sea surface temperature and sea ice cover, in combination with the aerosol  
24 emissions from the Representative Concentration Pathways (RCPs) scenarios. We find  
25 that the global annual mean aerosol net cooling effect at the top of the atmosphere  
26 (TOA) will be enhanced by  $0.12 \text{ W m}^{-2}$  compared with recent past year 2000 levels if  
27 the emissions of only BC are reduced to the level projected for 2100 based on the  
28 RCP2.6 scenario. This will be beneficial for the mitigation of global warming.  
29 However, both aerosol negative direct and indirect radiative effects are weakened  
30 when BC and its co-emitted species (sulfur dioxide and organic carbon) are  
31 simultaneously reduced. Relative to year 2000 levels, the global annual mean aerosol  
32 net cooling effect at the TOA will be weakened by  $1.7\text{--}2.0 \text{ W m}^{-2}$  if the emissions of  
33 all these aerosols are decreased to the levels projected for 2100 in different ways  
34 based on the RCP2.6, RCP4.5, and RCP8.5 scenarios. Because there are no effective  
35 ways to remove the BC exclusively without influencing the other co-emitted  
36 components, our results therefore indicate that a reduction in BC emission can lead to  
37 an unexpected warming on the Earth's climate system in the future.

38

## 39 **1 Introduction**

40 Aerosols in the atmosphere can alter the amount of sunlight reaching the Earth,  
41 perturb the temperature structure of the atmosphere, and influence cloud cover by  
42 directly scattering sunlight (e.g., sulphate, organic carbon (OC) and nitrate) or  
43 absorbing it (e.g., black carbon (BC) and dust) (Boucher et al., 2013). Aerosol  
44 particles can also change cloud microphysical and optical properties by acting as

45 cloud condensation nuclei (CCN) or ice nuclei (Twomey, 1977; Albrecht, 1989;  
46 DeMott et al., 1997). These changes due to aerosols will directly or indirectly affect  
47 the climate. Since the start of the industrial era, an increase in atmospheric aerosol  
48 emissions has likely led to a net cooling of the Earth's climate system (Boucher et al.,  
49 2013).

50 BC has a special role in the climate system, although it accounts for less than 5%  
51 of the mass of atmospheric aerosol in most areas of the world (X. Y. Zhang et al.,  
52 2012). BC can increase the amount of solar radiation absorbed within the Earth's  
53 climate system and heat the atmosphere or surface by directly absorbing sunlight in  
54 the visible to infrared wavebands (Hansen et al., 2000; Ramanathan and Carmichael,  
55 2008), changing the cloud amount and its brightness due to embedding into clouds  
56 (Chuang et al., 2002; Koch and Del Genio, 2010; Jacobson, 2012; Wang et al., 2013a),  
57 or by reducing the surface albedo due to deposition onto snow and ice surfaces (Wang  
58 et al., 2011; Lee et al., 2013). BC has even been considered as a potential cause of  
59 global warming (Hansen et al., 2000; Jacobson, 2010; Bond et al., 2013). Ramanathan  
60 and Carmichael (2008) compared the radiative forcings of greenhouse gases and BC,  
61 suggesting that the direct radiative forcing due to BC was larger than that due to any  
62 other greenhouse gas except CO<sub>2</sub>. The radiative heating effect on the whole  
63 atmosphere due to BC was almost double that due to all greenhouse gases. By  
64 considering all the known ways that BC affects the climate system, Bond et al. (2013)  
65 gave an estimate of industrial-era climate forcing of +1.1 W m<sup>-2</sup> due to BC with 90%  
66 uncertainty limits of +0.17 to +2.1 W m<sup>-2</sup>. BC can therefore be considered the second

67 most important anthropogenic positive radiative forcing agent after CO<sub>2</sub> in the  
68 present-day atmosphere. Some studies have even suggested that global warming could  
69 be slowed down in the short term by eliminating BC emission due to its short  
70 atmospheric lifetime. For example, eliminating soot generated from fossil fuels,  
71 including BC, primary organic matter, and sulphate, was found to decrease global  
72 surface air temperature by 0.3–0.5 °C in the short term (about 15 year) (Jacobson,  
73 2010). A simultaneous decrease of short-lived BC and methane through the adoption  
74 of control measures could reduce projected global mean warming by about 0.5 °C by  
75 2050 (Shindell et al., 2012). However, there is a huge uncertainty and an ongoing  
76 debate in climate forcing of BC. Other studies, such as Myhre et al. (2013a), have  
77 much lower estimate of the direct radiative forcing from BC, which is reflected in the  
78 best estimate in the latest IPCC report (Boucher et al., 2013; Myhre et al., 2013b).  
79 Recent literature also suggests that the climate effect of BC may be overestimated due  
80 to overestimation of its lifetime (e.g., Hodnebrog et al., 2014; Samset et al., 2014; Q.  
81 Wang et al., 2014).

82 Reducing the emissions of absorptive aerosols (e.g., BC) would decrease the  
83 absorption of solar radiation by atmospheric aerosols, thereby enhancing the aerosol  
84 net cooling effect. However, BC, OC, sulphate, and some other aerosols have many  
85 common emission sources (e.g., in the emission sectors of transportation, industrial,  
86 residential, and commercial energy consumption, etc.), and they are generally  
87 co-emitted into the atmosphere (Lamarque et al., 2010). A technology-based global  
88 emission inventory of BC and OC showed that BC and primary OC particles were

89 co-emitted from combustion including fossil fuels, biofuels, open biomass burning,  
90 and urban waste burning (Bond et al., 2004). An inventory of air pollutant emissions  
91 in Asia supporting the Intercontinental Chemical Transport Experiment-Phase B  
92 showed that sulfur dioxide (SO<sub>2</sub>), BC, and OC all were emitted from power, industry,  
93 residential, and transportation sources (Zhang et al., 2009). A spatially resolved  
94 biomass burning data set also indicated that BC, OC, and SO<sub>2</sub> were proportionally  
95 emitted from biofuel and forest fire sources (Reddy and Venkataraman, 2002).  
96 Analyses of aerosol emission trends from some important source regions showed that  
97 there were same trends for BC, OC, and SO<sub>2</sub> separately emitted from fossil fuel,  
98 biofuel, and biomass burning sources from 1980 to 2009 (Chin et al., 2014), which  
99 indirectly suggested the co-emissions of BC with some other aerosols. Moreover,  
100 actual operational reduction in BC emission in most of severe polluted countries, like  
101 China, is often to cut the usage of coal and other fossil fuels, as well as forbid open  
102 burning to reduce biomass burning emissions. All these major measures will result in  
103 the emission reductions in BC and its co-emitted components at the same time.

104 Sulphate, BC, and OC are the main aerosol species in the atmosphere, and the  
105 emissions of sulphate and OC will be reduced accordingly if the emission of BC is  
106 reduced. Both sulphate and OC are strongly scattering and hygroscopic aerosols, and  
107 they can cool the climate system by directly scattering solar radiation and increasing  
108 the cloud albedo and lifetime by acting as CCN (Boucher et al., 2013). Therefore,  
109 would global warming necessarily be slowed down by reducing BC emission in the  
110 future? This is the point of this study.

111 Focusing on the issue mentioned above, the impact of removing some BC sources  
112 and other co-emitted species on the aerosol radiative effects was studied in this paper  
113 by using an aerosol-climate atmosphere-only model  
114 BCC\_AGCM2.0.1\_CUACE/Aero (Atmospheric General Circulation Model of  
115 Beijing Climate Center, BCC\_AGCM2.0.1, coupled with the aerosol model of China  
116 Meteorological Administration Unified Atmospheric Chemistry Environment for  
117 Aerosols, CUACE/Aero) (Wang et al., 2014) with prescribed sea surface temperature  
118 (SST) and sea ice cover (SIC), in combination with the Representative Concentration  
119 Pathways (RCPs) emission scenarios (van Vuuren et al., 2011) underpinning the Fifth  
120 Assessment Report of the Intergovernmental Panel on Climate Change (IPCC AR5).  
121 In Sect. 2, we introduce the aerosol-climate model and simulation details. In Sect. 3,  
122 we present the effects of reducing only BC emission and then of the simultaneous  
123 reduction of BC and other co-emitted aerosol emissions on aerosol direct, semi-direct  
124 and indirect, and net radiative effects. Finally, our **discussion and conclusions** are  
125 presented in Sect. 4.

126

## 127 **2 Model and Simulation**

### 128 **2.1 Model description**

129 We use the aerosol-climate atmosphere-only model  
130 BCC\_AGCM2.0.1\_CUACE/Aero developed by Zhang et al. (2012a), and improved  
131 by Jing and Zhang (2013), Zhang et al. (2014), and Wang et al. (2014) in this study.  
132 The aerosol direct, semi-direct, and indirect effects (albedo and lifetime indirect

133 effects on stratiform clouds) have been included in BCC\_AGCM2.0.1\_CUACE/Aero.  
134 The model has been used to study the impact of aerosol direct radiative effect on East  
135 Asian climate (Zhang et al., 2012a), direct radiative forcing of anthropogenic aerosols  
136 (Bond et al., 2013; Myhre et al., 2013a), climate response to the presence of BC in  
137 cloud droplets (Wang et al., 2013a), effect of non-spherical dust aerosol on its direct  
138 radiative forcing (Wang et al., 2013b), anthropogenic aerosol indirect effect (Wang et  
139 al., 2014), and direct effect of dust aerosol on arid and semi-arid regions (Zhao et al.,  
140 2014).

141 A detailed description of BCC\_AGCM2.0.1 was given by Wu et al. (2010). The  
142 model employs a horizontal resolution of T42 (approximately  $2.8^\circ \times 2.8^\circ$ ) and a 26  
143 layer hybrid sigma-pressure coordinate system in the vertical direction, with a rigid lid  
144 at 2.9 hPa. The time step is 20 min. However, the cloud overlap, radiation, and cloud  
145 microphysical schemes were improved in the model. The cloud overlap scheme of the  
146 Monte Carlo independent column approximation (McICA) (Pincus et al., 2003) and  
147 the Beijing Climate Center RADiation transfer model (BCC\_RAD) developed by  
148 Zhang et al. (2003, 2006a, b) were used instead of the old schemes in the model (Jing  
149 and Zhang et al., 2013). These schemes have improved the accuracy of the subgrid  
150 cloud structure and its radiative transfer process (Zhang et al., 2014). A two-moment  
151 bulk cloud microphysical scheme to predict both the mass and number concentrations  
152 of cloud droplets and ice crystals (Morrison and Gettelman, 2008) was implemented  
153 into the model instead of the old one-moment bulk cloud microphysical scheme  
154 (Wang et al., 2014). The scheme of Abdul-Razzak and Ghan (2000) has been adopted

155 for the activation of cloud droplets.

156 The aerosol model CUACE/Aero is a comprehensive module incorporating  
157 emission, gaseous chemistry, transport, removal, and size-segregated  
158 multi-component aerosol algorithms based on the Canadian Aerosol Module  
159 developed by Gong et al. (2002, 2003). A detailed description of CUACE/Aero was  
160 given by Zhou et al. (2012). The mass concentrations of the main five aerosols in  
161 troposphere, i.e., sulphate, BC, OC, dust, and sea salt, can be calculated. Each aerosol  
162 type is divided into 12 bins as a geometric series for a radius between 0.005 and 20.48  
163  $\mu\text{m}$ . Aerosol optical properties from Wei and Zhang (2011) and Zhang et al. (2012b)  
164 were calculated based on the Mie theory. The refractive indices of aerosols were  
165 adopted from d'Almeida (1991). Hygroscopic growth was considered for sulphate,  
166 OC, and sea salt (Zhang et al., 2012a).

167

## 168 **2.2 Simulation details**

169 Six simulations were run in this study. In all simulations, the model settings were  
170 the same, whereas aerosol emissions were different. All simulations kept greenhouse  
171 gas concentrations fixed at year 2000 levels in order to obtain the effect of change in  
172 aerosol emissions exclusively. Table 1 gives the emission setups in all simulations. As  
173 a base case, the first simulation (SIM1) used emissions of  $\text{SO}_2$ , BC, and OC for the  
174 year 2000, representing the aerosol effect for recent past. In the second simulation  
175 (SIM2), BC emission in 2100 under the RCP2.6 scenario was used, but the emissions  
176 of  $\text{SO}_2$  and OC were the same as those in SIM1. In the third simulation (SIM3), BC



177 emission in 2100 under the RCP2.6 scenario was also used, but the emissions of SO<sub>2</sub>  
178 and OC used were those for 2100 under the RCP8.5 scenario. In the fourth simulation  
179 (SIM4), the emissions of SO<sub>2</sub>, BC, and OC for 2100 under the RCP2.6 scenario were  
180 used. In the fifth simulation (SIM5), BC emission in 2100 under the RCP2.6 scenario  
181 was used, but the emissions of SO<sub>2</sub> and OC used corresponded to the 2100 emission  
182 of BC under the RCP2.6 scenario by multiplying them with the ratios of the emissions  
183 of SO<sub>2</sub> and OC with BC in 2000. The ratios were calculated and applied for each  
184 individual grid box and month. In the sixth simulation (SIM6), the emissions of SO<sub>2</sub>,  
185 BC, and OC in 2100 under the RCP4.5 scenario were used. Aerosol emission  
186 inventories from fossil fuel, biofuel, and biomass burning for the year 2000 given by  
187 Lamarque et al. (2010) were used. The emission dataset of RCPs scenarios were  
188 described by van Vuuren et al. (2011) and can be obtained from  
189 <http://tntcat.iiasa.ac.at:8787/RcpDb/dsd?Action=htmlpage&page=about>. The biomass  
190 burning emissions are also changed when using RCPs scenarios. The National Centers  
191 for Environmental Prediction (NCEP) reanalysis climatological data on a Gaussian  
192 grid was used as the initial field (downloaded from  
193 <http://www.cesm.ucar.edu/models/atm-cam/download/>). Data for the prescribed  
194 annual cycle of monthly mean SST and SIC based on the 21-year (1981–2001)  
195 climatology from the Hadley Centre (Hurrell et al., 2008) were used in these  
196 simulations. Each simulation was run for 20 years, and the simulation data for the last  
197 10 years were averaged and analyzed.

198 The difference between SIM2 and SIM1 shows the impact on aerosol radiative

199 effects (AREs) of reducing only BC emission maximally in the four RCPs scenarios.  
200 The difference between SIM3 and SIM1 indicates the effect of maximally reducing  
201 the emission of absorbing BC, combined with the least reduction in the emissions of  
202 precursor (SO<sub>2</sub>) of scattering sulphate and OC on AREs. The differences between  
203 SIM4 and SIM1, between SIM5 and SIM1, and between SIM6 and SIM1 show the  
204 effects of a simultaneous reduction of SO<sub>2</sub>, BC, and OC emissions under the RCP2.6  
205 scenario, a reduction of the BC emission with a simultaneous reduction of the  
206 emissions of SO<sub>2</sub> and OC (in terms of their ratios with BC), and a simultaneous  
207 reduction in the emissions of SO<sub>2</sub>, BC, and OC under the RCP4.5 scenario  
208 (representing a medium-low emission pathway), on AREs, respectively.

209 The aerosol direct effect (ADE) was obtained by calling the radiation routine two  
210 times (Ghan et al., 2012):

$$211 \quad \Delta ADE = \Delta(F - F_{\text{clean}}), \quad (1)$$

212 where  $F$  is the radiative flux at the top of the atmosphere (TOA) and  $F_{\text{clean}}$  is the flux  
213 calculated as a diagnostic with aerosol scattering and absorption excluded;  $\Delta$  is the  
214 difference between 2000 and 2100. The change in cloud radiative forcing (CRF) was  
215 used as an approximate way of quantifying the change in combination of the aerosol  
216 semi-direct and indirect effects:

$$217 \quad \Delta CRF = \Delta(F - F_{\text{clear}}), \quad (2)$$

218 where  $F_{\text{clear}}$  is the flux calculated as a diagnostic with clouds neglected. The change in  
219 aerosol net effect was assessed by the change in net radiation flux at the TOA ( $\Delta F$ )  
220 (Ghan et al., 2012). We didn't perform additional simulations in which aerosol

221 scattering and absorption were neglected to exclusively diagnose the effect of aerosols  
222 on CRF according to the method by Ghan et al. (2012) and Ghan (2013). Thus, the  
223 difference in aerosol net effect is not equal to the sum of  $\Delta ADE$  and  $\Delta CRF$  in this  
224 study.

225

## 226 **3 Results**

### 227 **3.1 Aerosol optical depth for present-day conditions**

228 The simulation performance of BCC\_AGCM2.0.1\_CUACE/Aero has been given  
229 by Wang et al. (2014) in detail. They demonstrated that the model has a good ability  
230 to simulate aerosols, cloud properties, and meteorological fields. However, we replace  
231 the aerosol emission from AeroCom with those given by Lamarque et al. (2010) for  
232 present-day conditions in this work. Thus, a comparison of simulated annual mean  
233 aerosol optical depth (AOD) with satellite retrievals is shown in Figure 1. The  
234 simulated AODs range from 0.3 to 0.6 over the Sahara Desert and are from 0.15 to 0.3  
235 in nearby Arabian areas due to the large dust loading. The AODs are mainly between  
236 0.2 and 0.4 in eastern China, and exceed 0.15 in eastern North America and West  
237 Europe due to the large emissions of anthropogenic aerosols. The AODs are above 0.1  
238 over most subtropical oceans because of the contribution of sea salt and sulphate. The  
239 model generally reproduces the geographical distribution of AOD well, but it  
240 significantly underestimates the AODs over South Asia, eastern China, and tropical  
241 oceans. These errors could be caused by several factors such as uncertainties in the  
242 aerosol sources, coarse model resolution, the uncertainties of physical processes, and

243 the absence of nitrate, ammonium and secondary organic aerosols in the model  
244 (Zhang et al., 2012a).

245

## 246 **3.2 The effect of aerosol reductions**

### 247 **3.2.1 Global mean statistics**

248 Tables 2 and 3 show the global emission amounts and annual mean column  
249 burdens of aerosols in all simulations and differences in AREs among them. The  
250 global emission amount of BC is reduced from 7.8 Tg yr<sup>-1</sup> at present to 3.3 Tg yr<sup>-1</sup> at  
251 the end of this century under the RCP2.6 scenario due to the operation of various  
252 control measures. The global annual mean of simulated BC burden is decreased from  
253 0.17 mg m<sup>-2</sup> in SIM1 to 0.08 mg m<sup>-2</sup> in SIM2, assuming that only BC emission is  
254 reduced under the RCP2.6 scenario (Table 2). The reduction in the mass concentration  
255 of atmospheric BC results in less direct absorption of solar radiation by atmospheric  
256 aerosols, thereby causing the global annual mean aerosol direct radiative effect at the  
257 TOA to be enhanced by 0.07 W m<sup>-2</sup>. This indicates that the net cooling effect is  
258 enhanced. The multi-model comparison showed that our model had much lower  
259 normalized radiative forcing for BC than most of the other models (Myhre et al.,  
260 2013a). Thus, the change in aerosol direct radiative effect is quite small **despite** the  
261 strong emission reduction for BC. The reduction in the BC concentration also  
262 weakens the aerosol semi-direct effect, resulting in an increase of 0.11 W m<sup>-2</sup> in the  
263 absolute value of the global annual mean net CRF (Table 3). Of which, the shortwave  
264 cloud forcing (SWCF) and longwave cloud forcing (LWCF) **components** are

265 enhanced by 0.14 and 0.03  $\text{W m}^{-2}$ , respectively. It is noted that the change in CRF is a  
266 combined effect of decrease in cloud evaporation and increase in cloud cover caused  
267 by declining BC, changes in other aerosol concentrations due to adjustment of the  
268 atmosphere to BC reduction, and the resulting changes in cloud properties. However,  
269 the slight decrease in the sulphate mass concentration due to changes in  
270 meteorological fields caused by BC reduction partially offsets the net cooling effect in  
271 SIM2 compared with SIM1. Consequently, the global annual mean aerosol net cooling  
272 effect at the TOA is enhanced by 0.12  $\text{W m}^{-2}$  compared with recent past levels when  
273 just BC emission is reduced to the level projected for the end of this century under the  
274 RCP2.6 scenario (Table 3).

275 Many previous studies mentioned in Sect. 1 have indicated that there are several  
276 common sources of  $\text{SO}_2$ , BC, and OC (Reddy and Venkataraman, 2002; Zhang et al.,  
277 2009; Lamarque et al., 2010; Chin et al., 2014).  $\text{SO}_2$  and OC emissions are likely to  
278 be reduced proportionally when BC emission is decreased, as there is no effective  
279 way of removing BC exclusively without influencing the other co-emitted  
280 components. Therefore, we considered four different ways to simultaneously reduce  
281 the emissions of  $\text{SO}_2$ , BC, and OC to the levels projected for the end of this century  
282 under the RCP2.6, RCP4.5, and RCP8.5 scenarios. Then, we calculated the effects of  
283 emission reductions of all these aerosols on radiation fluxes in SIM3 to SIM6. It can  
284 be seen from Table 2 that the global emissions of  $\text{SO}_2$ , BC, and OC are decreased to  
285 12.9–25.7  $\text{Tg yr}^{-1}$ , 3.3–4.3  $\text{Tg yr}^{-1}$ , and 20.0–25.3  $\text{Tg yr}^{-1}$  under these three scenarios,  
286 respectively. Thus, the global annual mean burdens of sulphate, BC, and OC are

287 reduced by different levels (63–72, 51–55, and 25–31 %, respectively). The  
288 concurrent reductions in scattering sulphate and OC burdens weaken the global annual  
289 mean aerosol direct radiative effect at the TOA by  $0.25\text{--}0.3\text{ W m}^{-2}$ , although the  
290 absorbing BC burden is also significantly reduced in SIM3 to SIM6. Additionally,  
291 sulphate and OC particles can act as CCN due to their hygroscopicity, so any decrease  
292 in their emissions would decrease CCN concentrations, then decreasing cloud lifetime  
293 and albedo, thereby weakening the **negative** SWCF. As can be seen from Table 3, **the**  
294 **absolute values of** the global annual mean SWCF are weakened by  $0.87\text{--}1.3\text{ W m}^{-2}$   
295 due to simultaneous reductions in emissions of  $\text{SO}_2$ , BC, and OC. The quick  
296 adjustment of the atmosphere to aerosol effects leads to changes in LWCF, causing the  
297 longwave cooling by  $0.07\text{--}0.2\text{ W m}^{-2}$  in SIM3 to SIM6 compared with SIM1. It partly  
298 **offsets** the shortwave warming. The absolute values of global annual mean net CRF  
299 are decreased by  $0.8\text{--}1.1\text{ W m}^{-2}$  in SIM3 to SIM6 compared with SIM1, which greatly  
300 exceed the changes in the aerosol direct radiative effect. This is consistent with results  
301 obtained by Chen et al. (2010), who reported that a reduction in BC emission would  
302 dampen aerosol indirect forcing. Finally, the global annual mean aerosol net cooling  
303 effect at the TOA is weakened by  $1.7\text{--}2.0\text{ W m}^{-2}$  when the emissions of  $\text{SO}_2$ , BC, and  
304 OC are simultaneously reduced to the levels projected for the end of this century  
305 based on three different RCP scenarios (Table 3).

306

### 307 **3.2.2 Global distributions**

308 Figure 2 shows the global distributions of simulated annual mean sulphate, BC,

309 and OC burdens under all six simulations. As can be seen from Figure 2b, the BC  
310 column burdens are significantly decreased in areas with high BC emission such as  
311 East Asia, South Asia, central Africa and South America, eastern North America, and  
312 Western Europe compared with recent past levels when the emission of only BC is  
313 reduced. Changes in other aerosol burdens are not obvious. The reduction in the BC  
314 concentration weakens the direct absorption of solar radiation by atmospheric aerosols,  
315 leading to a cooling effect at the TOA in these regions. The largest cooling exceeds 1  
316  $\text{W m}^{-2}$  in China, Europe, and eastern North America (Fig. 3a). The numbers of  
317 activated sulphate, OC, and dust particles are increased over East and South Asia,  
318 Mediterranean regions, North America and Africa due to the fast adjustment in  
319 meteorological fields caused by declining BC (figure not shown), which leads to the  
320 increase in CCN concentration (Fig. 4a). Higher CCN concentrations can produce  
321 more cloud droplet numbers, with the maximum increase in annual mean column  
322 cloud droplet number concentrations (CDNCs) being up to  $0.6 \times 10^{10} \text{ m}^{-2}$  (Fig. 5a).  
323 This enhances the negative SWCF over those regions (Fig. 6a). In addition, the  
324 decrease in the absorption ability of aerosols weakens the cloud evaporation and  
325 increases the cloud fraction, which further enhances the negative SWCF over the  
326 regions with high BC emission and some oceans (Fig. 6a). However, the LWCF is  
327 also increased over most areas with enhanced negative SWCF (Fig. 6a), which can  
328 partly offset the shortwave cooling. Finally, only the reduction of BC emission results  
329 in an increase of more than  $2 \text{ W m}^{-2}$  in the annual mean aerosol net cooling effect at  
330 the TOA over most regions with large BC emission (Fig. 7a).

331 Figures 2c–f show that there are different levels of reduction in the annual mean  
332 sulphate, BC, and OC burdens in SIM3 to SIM6, with decreases of up to 2.0–5.0 mg S  
333 m<sup>-2</sup>, 0.2–1.0 mg m<sup>-2</sup> and 2.0–6.0 mg m<sup>-2</sup> in most areas, respectively, when all aerosol  
334 emissions are reduced. The combined reduction in scattering and absorbing aerosols  
335 weakens the aerosol direct radiative effect at the TOA by over 1 W m<sup>-2</sup> for most of the  
336 Northern Hemisphere (NH) compared with SIM1 (Fig. 3b–e). The CCN  
337 concentrations are greatly decreased over the globe, except for individual regions,  
338 mainly due to the emission reductions in hygroscopic sulphate and OC, especially  
339 over the middle latitudes of the NH (Fig. 4b–e). Correspondingly, the CDNCs are  
340 significantly decreased in SIM3 to SIM6 compared with SIM1. The largest decreases  
341 in annual mean column CDNCs exceed  $5 \times 10^{10}$  m<sup>-2</sup> in Western Europe, North  
342 America, and eastern China (Fig. 5b–e). Decreased CDNCs can decrease the cloud  
343 albedo and lifetime and weaken the negative SWCF in the regions with high  
344 anthropogenic aerosol emissions such as North America and Europe (Fig. 6b–e). The  
345 negative SWCFs are enhanced due to the increase in low cloud fraction over most of  
346 South and East Asia, though the CCNs are clearly decreased. The shortwave  
347 warmings (coolings) are also compensated by the longwave coolings (warmings) over  
348 most regions (Fig. 6b–e). Finally, the annual mean aerosol net cooling effect at the  
349 TOA is weakened over a range of 2.0–10.0 W m<sup>-2</sup> due to the changes in emissions of  
350 all aerosols over most regions of the NH that have large anthropogenic aerosol  
351 emissions (Fig. 7b–e).

352



#### 353 **4 Discussion and conclusions**

354 It has been argued that eliminating BC emission would be an effective measure  
355 to slow down global warming and environmental pollution. In this study, we assess  
356 the impact of removing some sources of BC and other co-emitted species on aerosol  
357 radiative effects by using an aerosol-climate atmosphere-only model  
358 BCC\_AGCM2.0.1\_CUACE/Aero with prescribed SST and SIC, in combination with  
359 the RCP scenarios. Compared with the aerosol effect for recent past, the global annual  
360 mean aerosol net cooling effect at the TOA is enhanced by  $0.12 \text{ W m}^{-2}$  due to a  
361 decrease in the direct absorption of solar radiation and aerosol semi-direct effect when  
362 BC emission is reduced exclusively to the level projected for the end of this century  
363 under the RCP2.6 scenario. The annual mean aerosol net cooling effect at the TOA is  
364 enhanced by more than  $2.0 \text{ W m}^{-2}$  in eastern China, northern India, and  
365 Mediterranean regions. Therefore, a reduction of BC emission alone could ideally  
366 mitigate global warming.

367 However, our results suggest that associating with the reduction of net cooling  
368 effects directly from aerosols, the aerosol indirect effect is also weakened when  
369 emissions of  $\text{SO}_2$ , BC, and OC are simultaneously reduced in different ways to the  
370 levels projected for the end of this century under the RCP2.6, RCP4.5, and RCP8.5  
371 scenarios. Relative to the aerosol effect for recent past, the total global annual mean  
372 aerosol net cooling effect at the TOA is weakened by  $1.7\text{--}2.0 \text{ W m}^{-2}$  with the  
373 reduction according to potential actual conditions in the emission of all these aerosols  
374 (i.e., BC and the major co-emitted species). The main cooling regions are over East

375 Asia, Western Europe, eastern North America, and central Africa, with the largest  
376 change exceeding  $10.0 \text{ W m}^{-2}$ . This is somewhat consistent with the results given by  
377 Gillett and Salzen (2013) and Levy et al. (2013), who also reported that the reduction  
378 in atmospheric aerosols will weaken the aerosol cooling effect in the future.

379 This study highlights that reducing only BC emission could play a positive role  
380 in mitigating global warming and environmental pollution, and would be beneficial to  
381 human health. However, the emissions of some co-emitted scattering aerosols and  
382 their precursor gases will be inevitably reduced when BC emission is reduced due to  
383 their homology. Therefore, reducing BC emission could lead to unexpected warming  
384 on the Earth's climate in the future, unless certain technical advances in emission  
385 reduction technology are available for removal of the BC exclusively without  
386 influencing the other co-emitted components.

387 There exists large uncertainty in BC radiative forcing (Bond et al., 2013;  
388 Boucher et al., 2013; Myhre et al., 2013a, 2013b). One reason for the uncertainty is  
389 from the biases of current emission inventories of BC, mostly obtained from the  
390 so-called bottom-up approach (Cohen and Wang, 2014). Cohen and Wang (2014)  
391 provided a global-scale top-down estimation of BC emissions, a factor of more than 2  
392 higher than commonly used global BC emissions data sets, by using a Kalman Filter  
393 method. If present-day BC emissions have been substantially underestimated, increase  
394 in aerosol net cooling effect may be larger due to only reduction in BC emission.  
395 Furthermore, co-emissions of other compounds with BC, such as  $\text{CO}_2$ , might be more  
396 important than  $\text{SO}_2$  and OC (Rogelj et al., 2014). The reduction in  $\text{CO}_2$  can mitigate

397 global warming when reducing BC. However, it is very difficult to fully obtain the  
398 ratios of BC with its co-emitted components due to the complexity of emission  
399 sources and diversity of energy structure in different regions. These bring about large  
400 uncertainties for the relevant research.

401 Because of the potential uncertainties mentioned above, we need to ongoingly  
402 improve our understanding on emissions of BC and its co-emitted species through a  
403 lot of observation and analysis. We also encourage other modeling groups to perform  
404 similar simulations to check the robustness of these results.

405

406 *Acknowledgments.* This work was supported by the National Basic Research Program  
407 of China (2011CB403405), National Natural Science Foundation of China  
408 (41205116), Public Meteorology Special Foundation of MOST (GYHY201406023),  
409 MOST (2014BAC16B01), and CAMS Basis Research Project (2012Y003).

410

411

412

413

414

415

416

417

418

419 **Reference**

- 420 Abdul-Razzak, H. and Ghan, S. J.: A parameterization of aerosol activation 2.  
421 Multiple aerosol types, *J. Geophys. Res.*, 105, 6837–6844,  
422 doi:10.1029/1999JD901161, 2000.
- 423 Albrecht, B.: Aerosols, cloud microphysics, and fractional cloudiness, *Science*, 245,  
424 1227–1230, doi:10.1126/science.245.4923.1227, 1989.
- 425 Bond, T. C., Streets, D. G., Yarber, K. F., Nelson, S. M., Woo, J.-H., and Klimont, Z.:  
426 A technology-based global inventory of black and organic carbon emissions from  
427 combustion, *J. Geophys. Res.*, 109, D14203, doi:10.1029/2003JD003697, 2004.
- 428 Bond, T. C., Doherty, S. J., Fahey, D. W., Forster, P. M., Berntsen, T., DeAngelo, B. J.,  
429 Flanner, M. G., Ghan, S., Kärcher, B., Koch, D., Kinne, S., Kondo, Y., Quinn, P.  
430 K., Sarofim, M. C., Schultz, M. G., Schulz, M., Venkataraman, C., Zhang, H.,  
431 Zhang, S., Bellouin, N., Guttikunda, S. K., Hopke, P. K., Jacobson, M. Z., Kaiser,  
432 J. W., Klimont, Z., Lohmann, U., Schwarz, J. P., Shindell, D., Storelvmo, T.,  
433 Warren, S. G., and Zender, C. S.: Bounding the role of black carbon in the climate  
434 system: a scientific assessment, *J. Geophys. Res.-Atmos.*, 118, 1–173,  
435 doi:10.1002/jgrd.50171, 2013.
- 436 Boucher, O., Randall, D., Artaxo, P., Bretherton, C., Feingold, G., Forster, P.,  
437 Kerminen, V.-M., Kondo, Y., Liao, H., Lohmann, U., Rasch, P., Satheesh, S. K.,  
438 Sherwood, S., Stevens, B., and Zhang, X. Y.: Clouds and aerosols, in: *Climate*  
439 *Change 2013: The Physical Science Basis. Contribution of Working Group I to the*  
440 *Fifth Assessment Report of the Intergovernmental Panel on Climate Change*,

441 edited by: Stocker, T. F., Qin, D., Plattner, G.-K., Tignor, M., Allen, S. K.,  
442 Boschung, J., Nauels, A., Xia, Y., Bex, V., and Midgley, P. M., Cambridge Univ.  
443 Press, Cambridge, UK, New York, NY, USA, 573–632, 2013.

444 Chen, W.-T., Lee, Y. H., Adams, P. J., Nenes, A., and Seinfeld, J. H.: Will black  
445 carbon mitigation dampen aerosol indirect forcing?, *Geophys. Res. Lett.*, 37,  
446 L09801, doi:10.1029/2010GL042886, 2010.

447 Chin, M., Diehl, T., Tan, Q., Prospero, J. M., Kahn, R. A., Remer, L. A., Yu, H.,  
448 Sayer, A. M., Bian, H., Geogdzhayev, I. V., Holben, B. N., Howell, S. G.,  
449 Huebert, B. J., Hsu, N. C., Kim, D., Kucsera, T. L., Levy, R. C.,  
450 Mishchenko, M. I., Pan, X., Quinn, P. K., Schuster, G. L., Streets, D. G.,  
451 Strode, S. A., Torres, O., and Zhao, X.-P.: Multi-decadal aerosol variations from  
452 1980 to 2009: a perspective from observations and a global model, *Atmos. Chem.*  
453 *Phys.*, 14, 3657-3690, doi:10.5194/acp-14-3657-2014, 2014.

454 Chuang, C. C., Penner, J. E., Prospero, J. M., Grant, K. E., Rau, G. H., and Kawamoto,  
455 K.: Cloud susceptibility and the first aerosol indirect forcing: sensitivity to black  
456 carbon and aerosol concentrations, *J. Geophys. Res.*, 107, 4564,  
457 doi:10.1029/2000JD000215, 2002.

458 Cohen, J. B. and Wang, C.: Estimating global black carbon emissions using a  
459 top-down Kalman Filter approach, *J. Geophys. Res.-Atmos.*, 119, 307–323,  
460 doi:10.1002/2013JD019912, 2014.

461 d’Almeida, G. A., Koepke, P., and Shettle, E.: *Atmospheric Aerosols: Global*  
462 *Climatology and Radiative Forcing*, 561 pp., A. Deepak, Hampton, Va, 1991.

463 DeMott, P. J., Rogers, D. C., and Kreidenweis, S. M.: The susceptibility of ice  
464 formation in upper tropospheric clouds to insoluble aerosol components, *J.*  
465 *Geophys. Res.*, 102, 19575–19584, doi:10.1029/97JD01138, 1997.

466 Ghan, S. J., Liu, X., Easter, R. C., Zaveri, R., Rasch, P. J., Yoon, J.-H., and Eaton, B.:  
467 Toward a minimal representation of aerosols in climate models: Comparative  
468 decomposition of aerosol direct, semi-direct and indirect radiative forcing, *J.*  
469 *Climate*, 25, 6461–6476, doi:10.1175/JCLI-D-11-00650.1, 2012.

470 Ghan, S. J.: Technical Note: Estimating aerosol effects on cloud radiative forcing,  
471 *Atmos. Chem. Phys.*, 13, 9971–9974, doi:10.5194/acp-13-9971-2013, 2013.

472 Gong, S. L., Barrie, L. A., and Lazare, M.: Canadian Aerosol Module (CAM): a  
473 size-segregated simulation of atmospheric aerosol processes for climate and air  
474 quality models, 2. Global seasalt aerosol and its budgets, *J. Geophys. Res.*, 107,  
475 4779, doi:10.1029/2001JD002004, 2002.

476 Gong, S. L., Barrie, L. A., Blanchet, J.-P., Salzen, K. V., Lohmann, U., Lesins, G.,  
477 Spacek, L., Zhang, L. M., Girard, E., Lin, H., Leaitch, R., Leighton, H., Chylek, P.,  
478 and Huang, P.: Canadian Aerosol Module: a size-segregated simulation of  
479 atmospheric aerosol processes for climate and air quality models 1. Module  
480 development, *J. Geophys. Res.*, 108, 4007, doi:10.1029/2001JD002002, 2003.

481 Gillett, N. P. and Salzen, K. V.: The role of reduced aerosol precursor emissions in  
482 driving near-term warming, *Environ. Res. Lett.*, 8, 034008,  
483 doi:10.1088/1748-9326/8/3/034008, 2013.

484 Hansen, J., Sato, M., Ruedy, R., Lacis, A., and Oinas, V.: Global warming in the

485 twenty-first century: an alternative scenario, *P. Natl. Acad. Sci. USA*, 97,  
486 9875–9880, 2000.

487 Hodnebrog, Ø., Myhre, G., and Samset, B. H.: How shorter black carbon lifetime  
488 alters its climate effect, *Nature Communications*, 5, 5065,  
489 doi:10.1038/ncomm6065, 2014.

490 Jacobson, M. Z.: Short-term effects of controlling fossil-fuel soot, biofuel soot and  
491 gases, and methane on climate, Arctic ice, and air pollution health, *J. Geophys.*  
492 *Res.*, 115, D14209, doi:10.1029/2009JD013795, 2010.

493 Jacobson, M. Z.: Investigating cloud absorption effects: Global absorption properties  
494 of black carbon, tar balls, and soil dust in clouds and aerosols, *J. Geophys. Res.*,  
495 117, D06205, doi:10.1029/2011JD017218, 2012.

496 Hurrell, J. W., Hack, J. J., Shea, D., Caron, J. M., and Rosinski, J.: A new sea surface  
497 temperature and sea ice boundary dataset for the Community Atmosphere Model.  
498 *J. Climate*, 21, 5145–5153, 2008.

499 Jing, X. and Zhang, H.: Application and evaluation of McICA scheme in  
500 BCC\_AGCM2.0.1, *AIP Conf. Proc.*, 1531, 756, doi:10.1063/1.4804880, 2013.

501 Koch, D. and Del Genio, A. D.: Black carbon semi-direct effects on cloud cover:  
502 review and synthesis, *Atmos. Chem. Phys.*, 10, 7685–7696,  
503 doi:10.5194/acp-10-7685-2010, 2010.

504 Lamarque, J.-F., Bond, T. C., Eyring, V., Granier, C., Heil, A., Klimont, Z., Lee, D.,  
505 Liousse, C., Mieville, A., Owen, B., Schultz, M. G., Shindell, D., Smith, S. J.,  
506 Stehfest, E., Van Aardenne, J., Cooper, O. R., Kainuma, M., Mahowald, N.,

507 McConnell, J. R., Naik, V., Riahi, K., and van Vuuren, D. P.: Historical  
508 (1850–2000) gridded anthropogenic and biomass burning emissions of reactive  
509 gases and aerosols: methodology and application, *Atmos. Chem. Phys.*, 10,  
510 7017–7039, doi:10.5194/acp-10-7017-2010, 2010.

511 Lee, Y. H., Lamarque, J.-F., Flanner, M. G., Jiao, C., Shindell, D. T., Berntsen, T.,  
512 Bisiaux, M. M., Cao, J., Collins, W. J., Curran, M., Edwards, R., Faluvegi, G.,  
513 Ghan, S., Horowitz, L. W., McConnell, J. R., Ming, J., Myhre, G., Nagashima, T.,  
514 Naik, V., Rumbold, S. T., Skeie, R. B., Sudo, K., Takemura, T., Thevenon, F.,  
515 Xu, B., and Yoon, J.-H.: Evaluation of preindustrial to present-day black carbon  
516 and its albedo forcing from Atmospheric Chemistry and Climate Model  
517 Intercomparison Project (ACCMIP), *Atmos. Chem. Phys.*, 13, 2607–2634,  
518 doi:10.5194/acp-13-2607-2013, 2013.

519 Levy, H., Horowitz, L. W., Schwarzkopf, M. D., Ming, Y., Golaz, J.-C., Naik, V., and  
520 Ramaswamy, V.: The roles of aerosol direct and indirect effects in past and future  
521 climate change, *J. Geophys. Res.-Atmos.*, 118, 4521–4532,  
522 doi:10.1002/jgrd.50192, 2013.

523 Morrison, H. and Gettelman, A.: A new two-moment bulk stratiform cloud  
524 microphysics scheme in the Community Atmosphere Model, version 3 (CAM3).  
525 part I: description and numerical tests, *J. Climate*, 21, 3642–3659, 2008.

526 Myhre, G., Samset, B. H., Schulz, M., Balkanski, Y., Bauer, S., Berntsen, T. K., Bian,  
527 H., Bellouin, N., Chin, M., Diehl, T., Easter, R. C., Feichter, J., Ghan, S. J.,  
528 Hauglustaine, D., Iversen, T., Kinne, S., Kirkevåg, A., Lamarque, J.-F., Lin, G.,



529 Liu, X., Lund, M. T., Luo, G., Ma, X., van Noije, T., Penner, J. E., Rasch, P. J.,  
530 Ruiz, A., Seland, Ø., Skeie, R. B., Stier, P., Takemura, T., Tsigaridis, K., Wang, P.,  
531 Wang, Z., Xu, L., Yu, H., Yu, F., Yoon, J.-H., Zhang, K., Zhang, H., and Zhou, C.:  
532 Radiative forcing of the direct aerosol effect from AeroCom Phase II simulations,  
533 Atmos. Chem. Phys., 13, 1853–1877, doi:10.5194/acp-13-1853-2013, 2013a.

534 Myhre, G., Shindell, D., Br éon, F.-M., Collins, W., Fuglestvedt, J., Huang, J., Koch,  
535 D., Lamarque, J.-F., Lee, D., Mendoza, B., Nakajima, T., Robock, A., Stephens, G.,  
536 Takemura, T., and Zhang, H.: Anthropogenic and natural radiative forcing, in:  
537 Climate Change 2013: The Physical Science Basis. Contribution of Working  
538 Group I to the Fifth Assessment Report of the Intergovernmental Panel on Climate  
539 Change, edited by: Stocker, T. F., Qin, D., Plattner, G.-K., Tignor, M., Allen, S. K.,  
540 Boschung, J., Nauels, A., Xia, Y., Bex, V., and Midgley, P. M., Cambridge Univ.  
541 Press, Cambridge, UK, New York, NY, USA, 659–740, 2013b.

542 Pincus, R., Barker, H. W., and Morcrette, J.-J.: A fast, flexible, approximate technique  
543 for computing radiative transfer in inhomogeneous cloud fields, J. Geophys. Res.,  
544 108, 4376, doi:10.1029/2002JD003322, 2003.

545 Ramanathan, V. and Carmichael, G.: Global and regional climate changes due to black  
546 carbon, Nature, 1, 221–227, 2008.

547 Reddy, S. M. and Venkataraman, C.: Inventory of aerosol and sulphur dioxide  
548 emissions from India: Part I – fossil fuel combustion, Atmos. Environ., 36,  
549 677–697, 2002.

550 Rogelj, J., Schaeffer, M., Meinshausen, M., Shindell, D. T., Hare, W., Klimont, Z.,

551 Velders, G. J. M., Amann, M., and Schellnhuber, H. J.: Disentangling the effects of  
552 CO<sub>2</sub> and short-lived climate forcer mitigation, *P. Natl. Acad. Sci. USA*, 111, 46,  
553 16325–16330, doi:10.1073/pnas.1415631111, 2014.

554 Samset, B. H., Myhre, G., Herber, A., Kondo, Y., Li, S.-M., Moteki, N., Koike, M.,  
555 Oshima, N., Schwarz, J. P., Balkanski, Y., Bauer, S. E., Bellouin, N., Bernsten, T.  
556 K., Bian, H., Chin, M., Diehl, T., Easter, R. C., Ghan, S. J., Iversen, T., Kirkevåg,  
557 A., Lamarque, J.-F., Lin, G., Liu, X., Penner, J. E., Schulz, M., Seland, Ø, Skeie, R.  
558 B., Stier, P., Takemura, T., Tsigaridis, K., and Zhang, K.: Modeled black carbon  
559 radiative forcing and atmospheric lifetime in AeroCom Phase II constrained by  
560 aircraft observations, *Atmos. Chem. Phys. Discuss.*, 14, 20083–20115,  
561 doi:10.5194/acpd-14-20083-2014, 2014.

562 Shindell, D., Kuylenstierna, J. C. I., Vignati, E., van Dingenen, R., Amann, M.,  
563 Klimont, Z., Anenberg, S. C., Muller, N., Janssens-Maenhout, G., Raes, F.,  
564 Schwartz, J., Faluvegi, G., Pozzoli, L., Kupiainen, K., Hoglund-Isaksson, L.,  
565 Emberson, L., Streets, D., Ramanathan, V., Hicks, K., Kim Oanh, N. T., Milly, G.,  
566 Williams, M., Demkine, V., and Fowler, D.: Simultaneously mitigating near-term  
567 climate change and improving human health and food security, *Science*, 335,  
568 183–189, doi:10.1126/science.1210026, 2012.

569 Twomey, S. A.: The influence of pollution on the shortwave albedo of clouds, *J.*  
570 *Atmos. Sci.*, 34, 1149–1152, 1977.

571 van Donkelaar, A., Martin, R. V., Brauer, M., Kahn, R., Levy, R., Verduzco, C., and  
572 Villeneuve, P. J.: Global estimates of ambient fine particulate matter

573 concentrations from satellite-based aerosol optical depth: Development and  
574 application, *Environ. Health Persp.*, 118, 847–855, doi:10.1289/ehp.0901623,  
575 2010.

576 van Vuuren, D. P., Edmonds, J., Kainuma, M., Riahi, K., Thomson, A., Hibbard, K.,  
577 Hurtt, G. C., Kram, T., Krey, V., and Lamarque, J.-F.: The representative  
578 concentration pathways: an overview, *Climatic Change*, 109, 5–31,  
579 doi:10.1007/s10584-011-0148-z, 2011.

580 Wang, Q., Jacob, D. J., Spackman, J. R., Perring, A. E., Schwarz, J. P., Moteki, N.,  
581 Marais, E. A., Ge, C., Wang, J., and Barrett, S. R. H.: Global budget and radiative  
582 forcing of black carbon aerosol: Constraints from pole-to-pole (HIPPO)  
583 observations across the Pacific, *J. Geophys. Res.-Atmos.*, 119, 1, 195–206,  
584 doi:10.1002/2013jd020824, 2014.

585 Wang, Z. L., Zhang, H., and Shen, X. S.: Radiative forcing and climate response due  
586 to black carbon in snow and ice, *Adv. Atmos. Sci.*, 28, 1336–1344,  
587 doi:10.1007/s00376-011-0117-5, 2011.

588 Wang, Z. L., Zhang, H., Li, J., Jing, X. W., and Lu, P.: Radiative forcing and climate  
589 response due to the presence of black carbon in cloud droplets, *J. Geophys. Res.*,  
590 118, 3662–3675, doi:10.1002/jgrd.50312, 2013a.

591 Wang, Z. L., Zhang, H., Jing, X. W., and Wei, X. D.: Effect of non-spherical dust  
592 aerosol on its direct radiative forcing, *Atmos. Res.*, 120, 112–126, doi:  
593 10.1016/j.atmosres.2012.08.006, 2013b.

594 Wang, Z. L., Zhang, H., and Lu, P.: Improvement of cloud microphysics in the

595 aerosol-climate model BCC\_AGCM2.0.1\_CUACE/Aero, evaluation against  
596 observations, and updated aerosol indirect effect, *J. Geophys. Res.*, 119,  
597 8400–8417, doi:10.1002/2014JD021886, 2014.

598 Wei, X. D. and Zhang, H.: Analysis of optical properties of nonspherical dust-like  
599 aerosols, *Acta Optica Sinica*, 31, 0501002-1–0501002-8,  
600 doi:10.3788/AOS201131.0501002, 2011.

601 Wu, T., Yu, R. C., Zhang, F., Wang, Z. Z., Dong, M., Wang, L., Jin, X., Chen, D., and  
602 Li, L.: The Beijing Climate Center atmospheric general circulation model:  
603 description and its performance for the present-day, *Clim. Dynam.*, 34, 123–147,  
604 doi:10.1007/s00382-009-0594-8, 2010.

605 Zhang, H., Nakajima, T., Shi G. Y., Suzuki, T., and Imasu, R.: An optimal approach to  
606 overlapping bands with correlated- $k$  distribution method and its application to  
607 radiative transfer calculations. *J. Geophys. Res.*, 108, 4641,  
608 doi:10.1029/2002JD003358, 2003.

609 Zhang, H., Shi, G. Y., Nakajima, T., and Suzuki, T.: The effects of the choice of the  
610  $k$ -interval number on radiative calculations, *J. Quant. Spectrosc. Ra.*, 98, 31–43,  
611 2006a.

612 Zhang, H., Suzuki, T., Nakajima, T., Shi, G. Y., Zhang, X. Y., and Liu, Y.: Effects of  
613 band division on radiative calculations. *Opt. Eng.*, 45, 016002,  
614 doi:10.1117/1.2160521, 2006b.

615 Zhang, H., Wang, Z. L., Wang, Z. Z., Liu, Q., Gong, S., Zhang, X. Y., Shen, Z., Lu, P.,  
616 Wei, X., Che, H., and Li, L.: Simulation of direct radiative forcing of typical

617 aerosols and their effects on global climate using an online AGCM-aerosol  
618 coupled model system, *Clim. Dynam.*, 38, 1675–1693, 2012a.

619 Zhang, H., Shen, Z. P., Wei, X. D., Zhang, M.-G., and Li, Z.: Comparison of optical  
620 properties of nitrate and sulfate aerosol and the direct radiative forcing due to  
621 nitrate in China, *Atmos. Res.*, 113, 113–125, 2012b.

622 Zhang, H., Jing, X. W., and Li, J.: Application and evaluation of a new radiation code  
623 under McICA scheme in BCC\_AGCM2.0.1, *Geosci. Model Dev.*, 7, 737–754,  
624 doi:10.5194/gmd-7-737-2014, 2014.

625 Zhang, Q., Streets, D. G., Carmichael, G. R., He, K. B., Huo, H., Kannari, A.,  
626 Klimont, Z., Park, I. S., Reddy, S., Fu, J. S., Chen, D., Duan, L., Lei, Y.,  
627 Wang, L. T., and Yao, Z. L.: Asian emissions in 2006 for the NASA INTEX-B  
628 mission, *Atmos. Chem. Phys.*, 9, 5131–5153, doi:10.5194/acp-9-5131-2009, 2009.

629 Zhang, X. Y., Wang, Y. Q., Niu, T., Zhang, X. C., Gong, S. L., Zhang, Y. M., and  
630 Sun, J. Y.: Atmospheric aerosol compositions in China: spatial/temporal variability,  
631 chemical signature, regional haze distribution and comparisons with global  
632 aerosols, *Atmos. Chem. Phys.*, 12, 779–799, doi:10.5194/acp-12-779-2012, 2012.

633 Zhao, S. Y., Zhang, H., Feng, S., and Fu, Q.: Simulating direct effects of dust aerosol  
634 on arid and semi-arid regions using an aerosol-climate coupled system, *Int. J.*  
635 *Climatol.*, doi:10.1002/joc.4093, 2014.

636 Zhou, C. H., Gong, S., Zhang, X.-Y., Liu, H. L., Xue, M., Cao, G. L., An, X. Q., Che,  
637 H. Z., Zhang, Y. M., and Niu, T.: Towards the improvements of simulating the  
638 chemical and optical properties of Chinese aerosols using an online coupled

639 model-CUACE/Aero, Tellus B, 64, 18965, 2012.

640

641

642

643

644

645

646

647

648

649

650

651

652

653

654

655

656

657

658

659

660

661 **Table 1.** Simulation setups.

Simulation	BC emission	OC & SO <sub>2</sub> emissions	Interpretation (compared to SIM1)
SIM1	year-2000	year-2000	Recent past reference emissions.
SIM2	RCP2.6 year-2100	year-2000	Maximal reduction in BC; no reductions in OC & SO <sub>2</sub> .
SIM3	RCP2.6 year-2100	RCP8.5 year-2100	Maximal reduction in BC; minimal reductions in OC & SO <sub>2</sub> .
SIM4	RCP2.6 year-2100	RCP2.6 year-2100	Simultaneous maximal reductions in BC, OC & SO <sub>2</sub> .
SIM5	RCP2.6 year-2100	RCP2.6 year-2100 BC by multiplying the ratios of the emissions of OC & SO <sub>2</sub> with BC in 2000	Maximal reduction in BC; simultaneous reductions of OC & SO <sub>2</sub> in terms of their ratios with BC in recent past
SIM6	RCP4.5 year-2100	RCP4.5 year-2100	Medium-low reductions in BC, OC & SO <sub>2</sub> .

662

663

664

665

666

667

668

669

670

671

672

673

674

675

676

677 **Table 2.** Global amounts of aerosol emissions and annual means of aerosol burdens.

	SIM1	SIM2	SIM3	SIM4	SIM5	SIM6
<b>Emission (Tg yr<sup>-1</sup>)</b>						
SO <sub>2</sub>	107.4	107.4	25.7	12.9	19.8	22.2
BC	7.8	3.3	3.3	3.3	3.3	4.3
OC	35.8	35.8	23.9	25.3	24.9	20.0
<b>Burden (mg m<sup>-2</sup>)</b>						
Sulphate	3.5	3.4	1.3	0.98	1.1	1.2
BC	0.17	0.079	0.078	0.077	0.078	0.084
OC	1.6	1.6	1.2	1.2	1.2	1.1
Dust	39.9	39.9	39.9	40.6	42.7	42.8
Sea salt	14.2	14.2	14.0	14.0	14.0	14.1

678

679

680

681

682

683

684

685

686

687

688

689

690

691

692

693



694 **Table 3.** Global annual mean differences of aerosol direct (DRF), semi-direct and  
 695 indirect (CRF), and net effect at the TOA (FNT) (Positive values mean incoming,  
 696 units:  $\text{W m}^{-2}$ ) in different simulations\* .

	SIM1	$\Delta$ SIM2	$\Delta$ SIM3	$\Delta$ SIM4	$\Delta$ SIM5	$\Delta$ SIM6
DRF	-2.01	-0.07 $\pm$ 0.05	+0.27 $\pm$ 0.03	+0.28 $\pm$ 0.05	+0.25 $\pm$ 0.03	+0.3 $\pm$ 0.02
SWCF	-49.0	-0.14 $\pm$ 0.2	+0.87 $\pm$ 0.3	+1.3 $\pm$ 0.14	+1.1 $\pm$ 0.17	+1.02 $\pm$ 0.2
LWCF	+27.8	+0.03 $\pm$ 0.09	-0.07 $\pm$ 0.08	-0.2 $\pm$ 0.1	-0.19 $\pm$ 0.08	-0.14 $\pm$ 0.1
CRF	-21.2	-0.11 $\pm$ 0.17	+0.8 $\pm$ 0.3	+1.1 $\pm$ 0.1	+0.91 $\pm$ 0.11	+0.88 $\pm$ 0.18
FNT	-0.66	-0.12 $\pm$ 0.28	+1.7 $\pm$ 0.2	+2.0 $\pm$ 0.19	+1.8 $\pm$ 0.14	+1.8 $\pm$ 0.21

697 \* DRF, SWCF, LWCF and CRF, and FNT in the SIM1 column are aerosol direct radiative forcing, shortwave, longwave and net  
 698 cloud radiative forcing, and net radiation flux at the TOA (units:  $\text{W m}^{-2}$ ) in SIM1, respectively. Values in the  $\Delta$ SIM2 –  $\Delta$ SIM6  
 699 columns represent the changes of corresponding variables in these simulations vs. those in SIM1.

700

701

702

703

704

705

706

707

708

709

710

711

712

713

714

715 **Figure captions:**

716 **Figure 1.** Global distributions of simulated and observed annual mean AOD at 550  
717 nm. (a) Simulation and (b) MODIS&MISR (van Donkelaar et al., 2010).

718 **Figure 2.** Global distributions of simulated annual mean aerosol column burdens  
719 (units:  $\text{mg m}^{-2}$ ).

720 **Figure 3.** Global distributions of difference in simulated annual mean aerosol direct  
721 effect (units:  $\text{W m}^{-2}$ ). (a) SIM2 – SIM1, (b) SIM3 – SIM1, (c) SIM4 – SIM1, (d)  
722 SIM5 – SIM1, and (e) SIM6 – SIM1.

723 **Figure 4.** Global distributions of difference in simulated annual mean CCN  
724 concentration at surface (units:  $\text{cm}^{-3}$ ). (a) SIM2 – SIM1, (b) SIM3 – SIM1, (c)  
725 SIM4 – SIM1, (d) SIM5 – SIM1, and (e) SIM6 – SIM1.

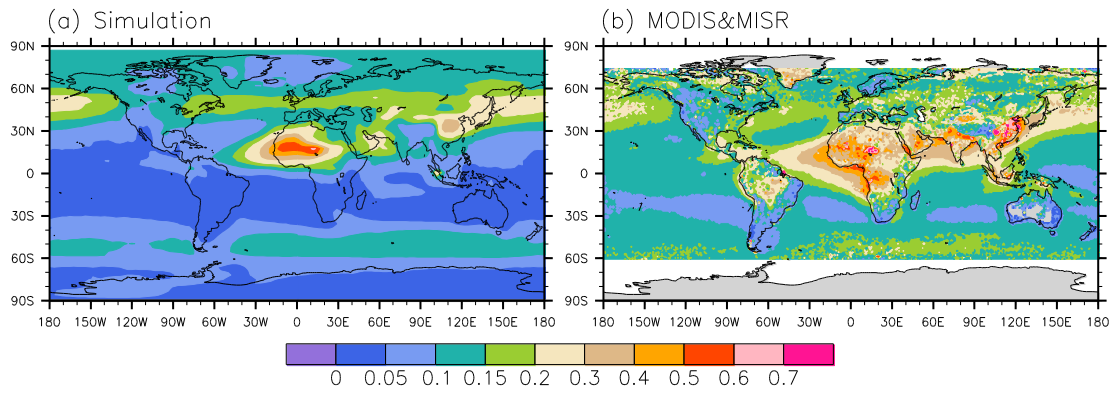
726 **Figure 5.** Global distributions of difference in simulated annual mean column CDNC  
727 (units:  $10^{10} \text{ m}^{-2}$ ). (a) SIM2 – SIM1, (b) SIM3 – SIM1, (c) SIM4 – SIM1, (d) SIM5  
728 – SIM1, and (e) SIM6 – SIM1.

729 **Figure 6.** Global distributions of difference in simulated annual mean SWCF and  
730 LWCF (units:  $\text{W m}^{-2}$ ). (a) SIM2 – SIM1, (b) SIM3 – SIM1, (c) SIM4 – SIM1, (d)  
731 SIM5 – SIM1, and (e) SIM6 – SIM1.

732 **Figure 7.** Global distributions of difference in simulated annual mean aerosol net  
733 effect (units:  $\text{W m}^{-2}$ ). (a) SIM2 – SIM1, (b) SIM3 – SIM1, (c) SIM4 – SIM1, (d)  
734 SIM5 – SIM1, and (e) SIM6 – SIM1.

735

736



737

738 **Figure 1.** Global distributions of simulated and observed annual mean AOD at 550

739 nm. (a) Simulation and (b) MODIS&MISR (van Donkelaar et al., 2010).

740

741

742

743

744

745

746

747

748

749

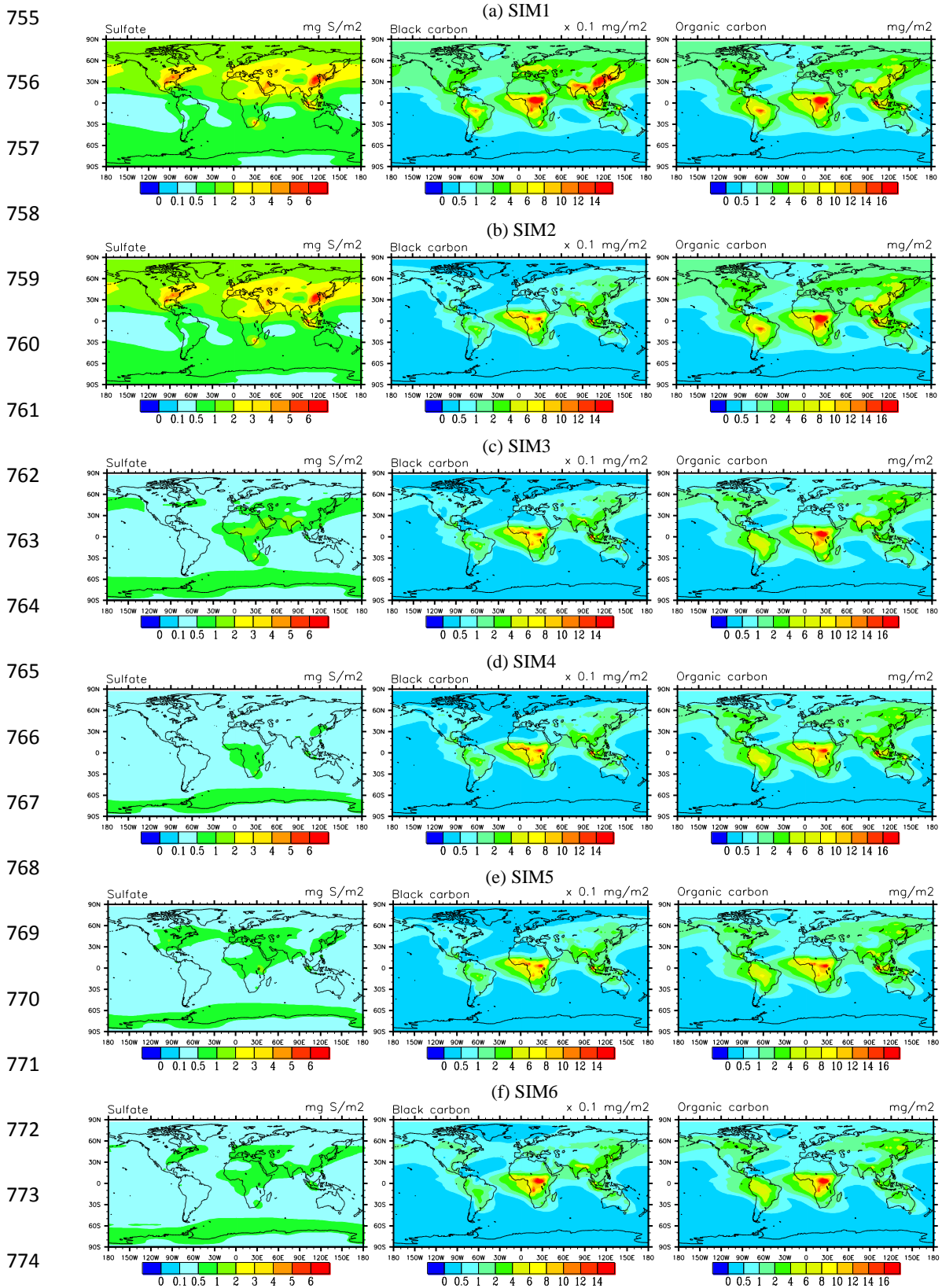
750

751

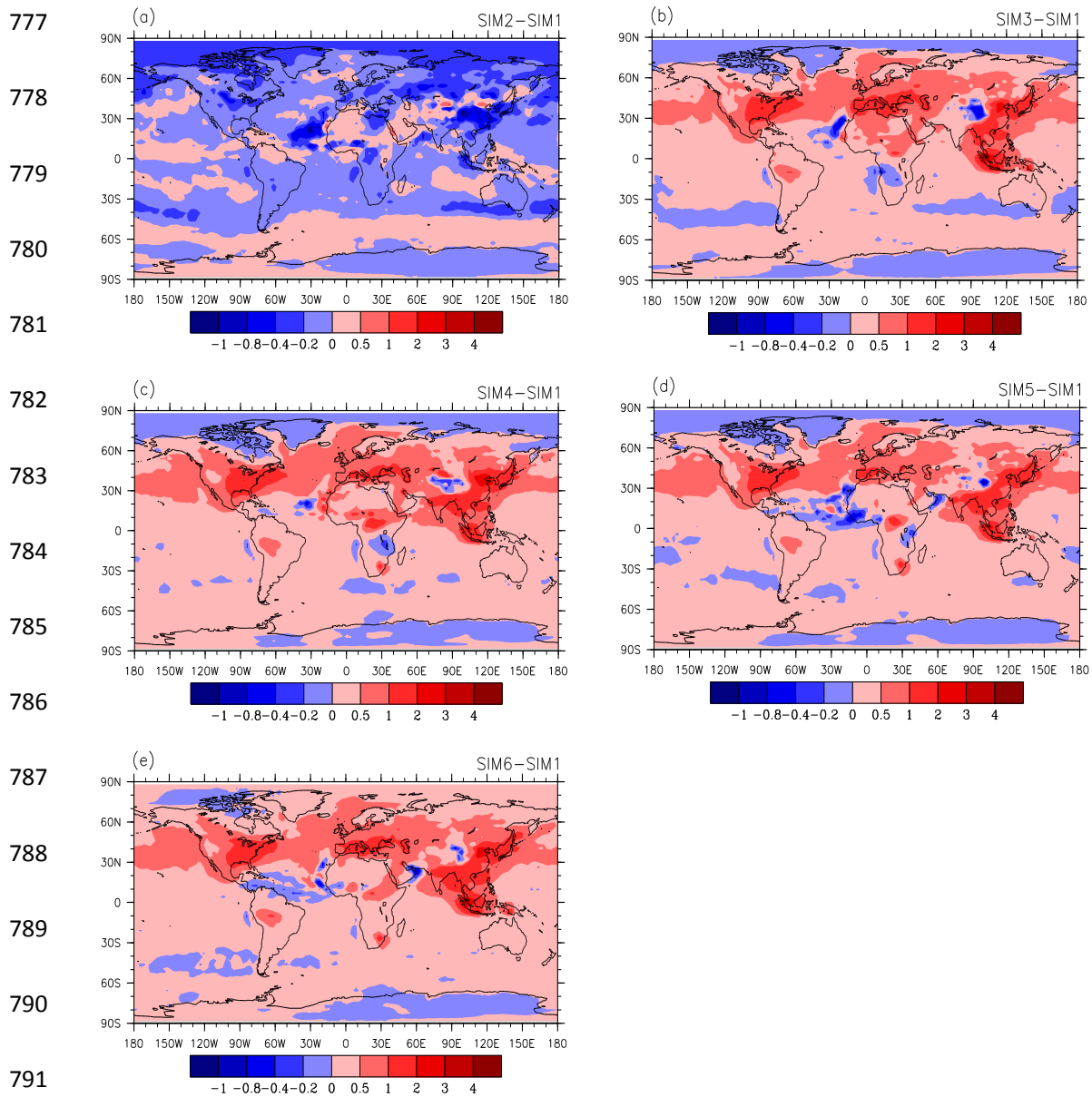
752

753

754

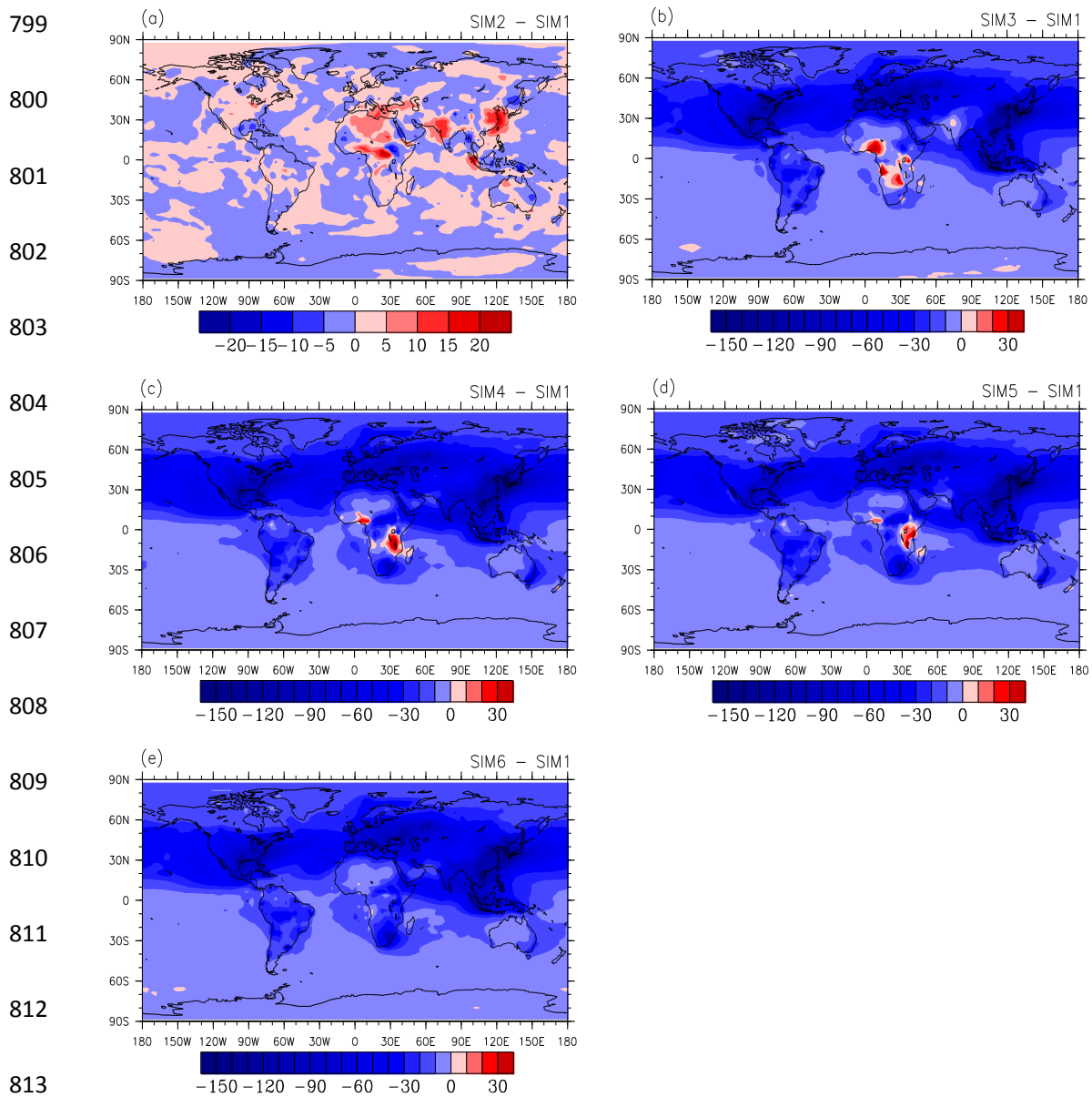


775 **Figure 2.** Global distributions of simulated annual mean aerosol column burdens  
 776 (units:  $\text{mg m}^{-2}$ ).



792 **Figure 3.** Global distributions of difference in simulated annual mean aerosol direct  
 793 effect (units:  $W m^{-2}$ ). (a) SIM2 – SIM1, (b) SIM3 – SIM1, (c) SIM4 – SIM1, (d)  
 794 SIM5 – SIM1, and (e) SIM6 – SIM1.

795  
 796  
 797  
 798



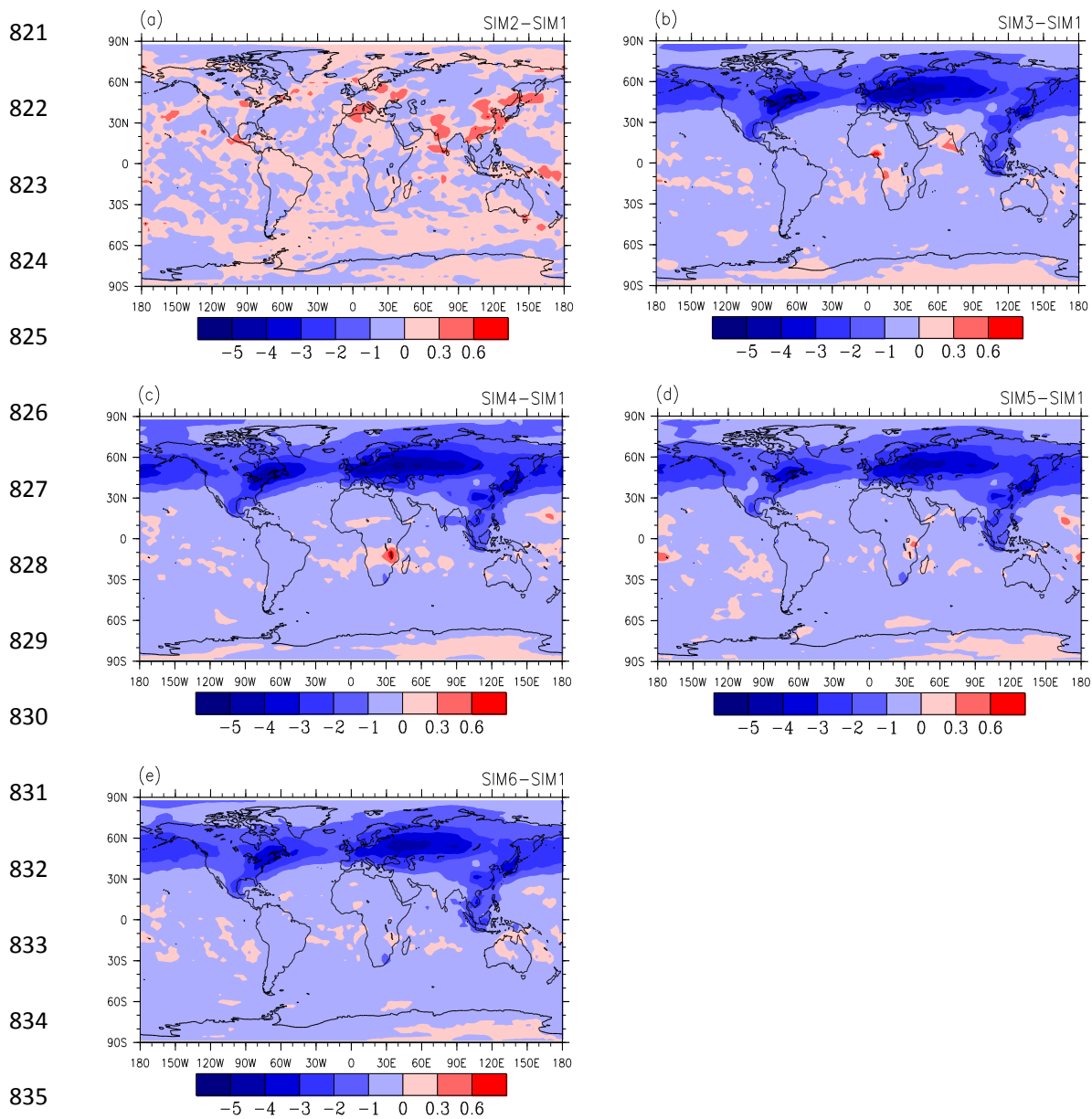
814 **Figure 4.** Global distributions of difference in simulated annual mean CCN  
 815 concentration at surface (units:  $\text{cm}^{-3}$ ). (a) SIM2 - SIM1, (b) SIM3 - SIM1, (c) SIM4  
 816 - SIM1, (d) SIM5 - SIM1, and (e) SIM6 - SIM1.

817

818

819

820

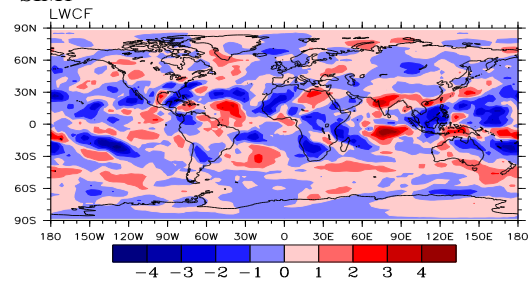
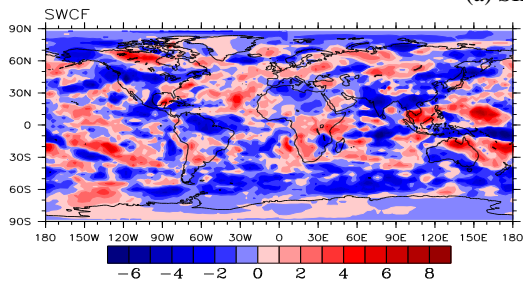


836 **Figure 5.** Global distributions of difference in simulated annual mean column CDNC  
 837 (units:  $10^{10} \text{ m}^{-2}$ ). (a) SIM2 – SIM1, (b) SIM3 – SIM1, (c) SIM4 – SIM1, (d) SIM5 –  
 838 SIM1, and (e) SIM6 – SIM1.

839  
 840  
 841  
 842

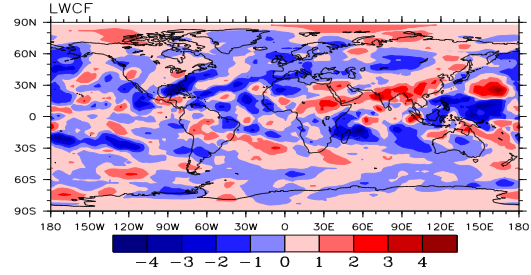
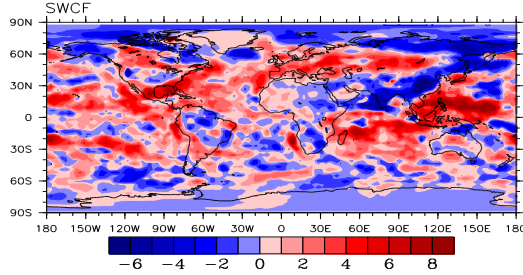
843

(a) SIM2 – SIM1



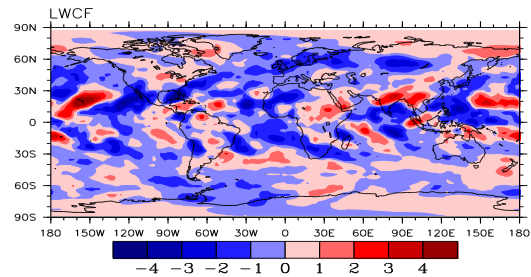
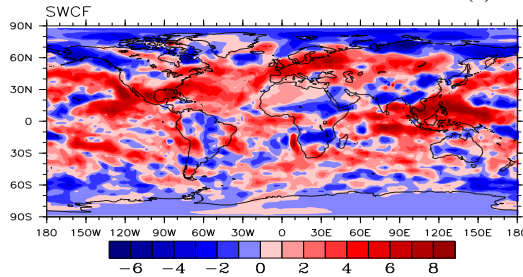
847

(b) SIM3 – SIM1



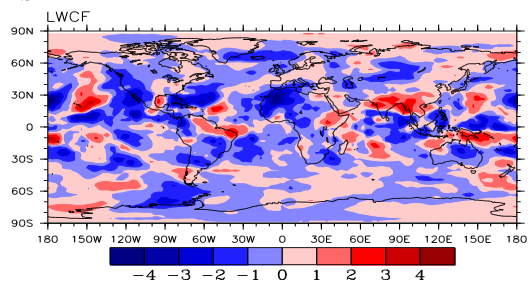
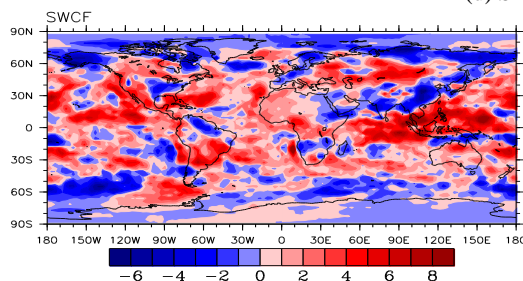
851

(c) SIM4 – SIM1



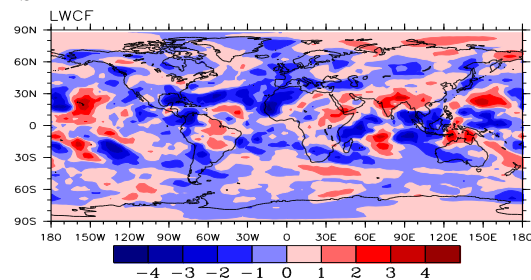
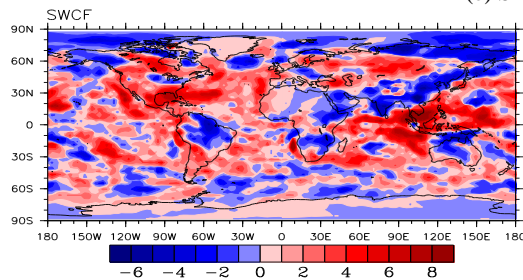
855

(d) SIM5 – SIM1



858

(e) SIM6 – SIM1

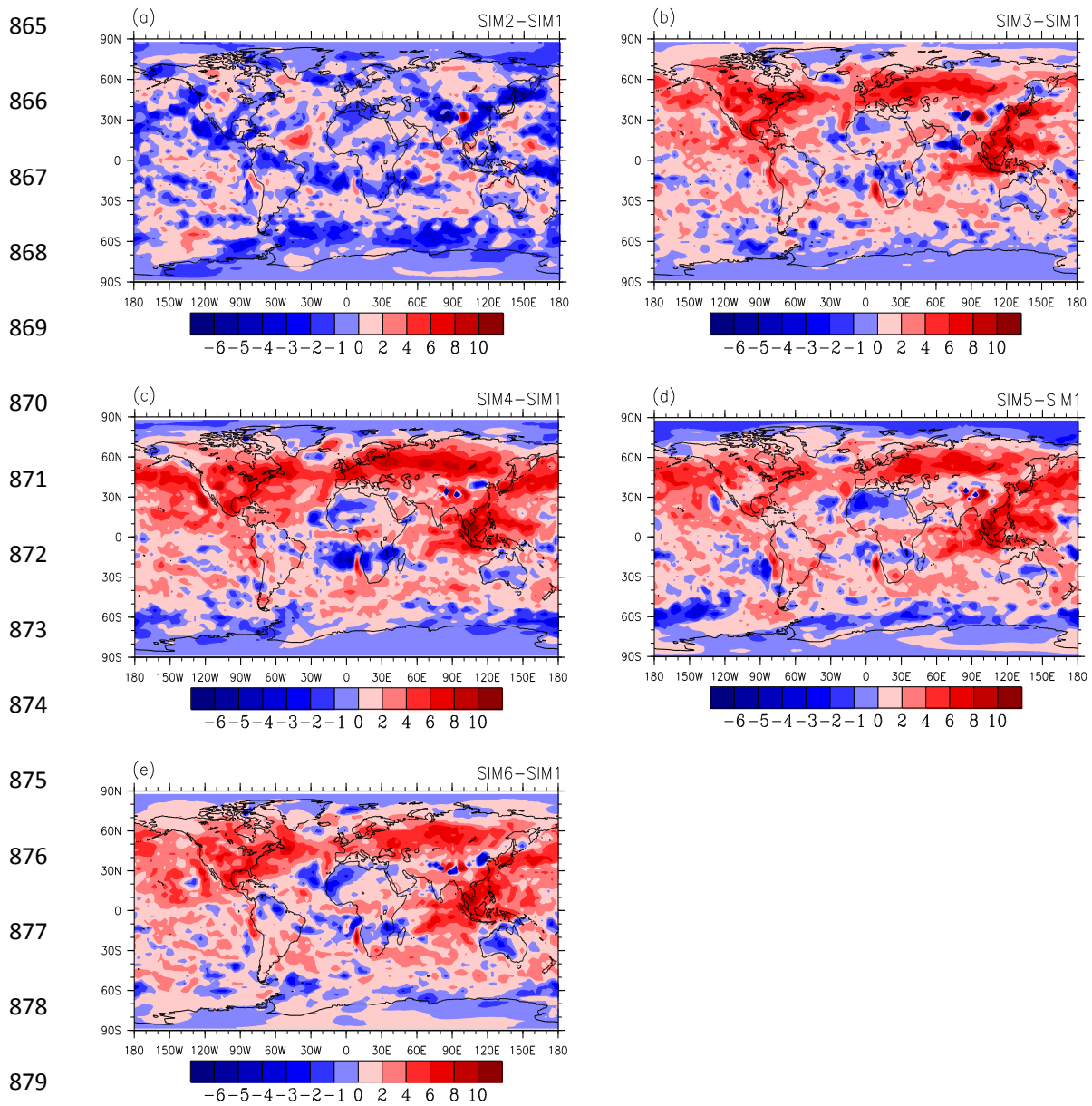


862 **Figure 6.** Global distributions of difference in simulated annual mean SWCF and

863 LWCF (units:  $W m^{-2}$ ). (a) SIM2 – SIM1, (b) SIM3 – SIM1, (c) SIM4 – SIM1, (d)

864 SIM5 – SIM1, and (e) SIM6 – SIM1.





880 **Figure 7.** Global distributions of difference in simulated annual mean aerosol net  
 881 effect (units:  $W m^{-2}$ ). (a) SIM2 – SIM1, (b) SIM3 – SIM1, (c) SIM4 – SIM1, (d)  
 882 SIM5 – SIM1, and (e) SIM6 – SIM1.